AISI H13 TOOL STEEL – COMPARISON BETWEEN POWDER BED FUSED AND CLASSICALLY PRODUCED PARTS

Samo TOME, Irena PAULIN, Matjaž GODEC

Institute of Metals and Technology, Ljubljana, Slovenia EU, samo.tome@imt.si

https://doi.org/10.37904/metal.2024.4881

Abstract

AISI H13 Is very commonly used in the hot-work category of steels. Whether it is used as a forging die, a hot-cutting tool, or a mold in injection molding or die casting, it is always on the table, as the material of choice. However, its potential has not yet been fully realized. New manufacturing techniques such as additive manufacturing (AM) broaden the horizon of the material's application, and promise improved performance, through optimized geometry, unobtainable by traditional means, and heightened mechanical properties. One of the more widespread AM processes is Powder Bed Fusion (PBF) where a laser or electron beam constructs the model, by meting a thin coating of metal powder applied to a base plate. By repeatedly applying and melting powder, the end result is a layer-by-layer produced part. However, the techniques for producing such parts are not yet refined enough and require further research. Problems like porosities, part deflection, and crack formation due to residual stress are commonplace, while comparably low mechanical properties in the as-processed state call for post-production treatments. Naturally, every technique has its boons and drawbacks, and that is what this work aims to analyze – How do the PBF parts compare to classically produced ones, and what are the difficulties in producing the later-mentioned parts.

Keywords: Powder bed fusion, Tool Steel, Additive Manufacturing, Mechanical Properties

1. INTRODUCTION

Additive manufacturing (AM) is a technique that is currently shaking up advanced manufacturing industries, such as aerospace, medical, and high-performance parts. However, the technique shows promise even in other, more well established industries. One of these is tool and die-making. Currently, most dies are made via subtractive methods, such as drilling or machining. One of the major limitations of this method is that cooling changes can only be drilled in mostly straight lines. This means that cooling of the die is nonoptimal, as hotspots may occur at certain parts of the tool. [1–3] Additive techniques such as laser powder bed fusion (LPBF) aim to amend that issue. Due to the nature of the process, it is possible to design tools with cooling channels, that conform to the shape of the die. This not only eliminates hot spots, but also lowers the amplitude of the temperature fluctuations, as the tool is in operation, reducing cycle times and extending tool life. [4,5] Another benefit AM provides is recyclability. While contemporary methods produce a significant amount of waste material, AM can reuse almost all of the unspent powder.

One of the most ubiquitous steels for die-making is AISI H13. It offers excellent hardness, and toughness at elevated temperatures, while also having high thermal fatigue and heat-softening resistance. [6,7] Therefore, it would make an excellent candidate for AM. However, despite AMs great potential in the tool-making world, there are still significant hurdles to overcome before its widespread adoption. Issues such as cracking and porosity significantly reduce the material's mechanical properties. [8,9] So, this paper aims to elucidate differences between classically produced and additively manufactured H13 parts.

2. MATERIALS AND EXPERIMENTAL PROCESS

The metal powder for this study was acquired from Carpenter Additive (Philadelphia, Pennsylvania). It has a median size of 45 µm and is produced via gas atomization. The steel for the conventionally produced parts was a bar of H13 produced by SIJ Metal Ravne (Ravne, Slovenia) and was in a soft annealed state. The chemical composition of both is given in **Table 1** and **Table 2**.

Table 1 Chemical composition of the SIJ Metal Ravne H13 steel bar

Element	C	Si	Mn	Cr	Mo	V
Mass %	0.4	1.05	0.40	5.15	1.35	1.00

Table 2 Chemical composition of the Carpenter additive H13 steel powder

B	C	Si	Mn	Cr	Mo	V
Mass %	0.35-0.42	0.80-1.20	0.25-0.50	4.80-5.50	1.10-1.50	0.80-1.15

2.1. Additively manufactured samples

The L-PBF samples were produced on an Aconity mini 3D printer with a preheating module. The samples were 15 mm x15 mm x 60 mm cubes (**Figure 1**). Due to the size limitations of the 100 mm radius base plate, the samples were manufactured in two batches. All samples were manufactured with 350 °C of preheating in an inert argon atmosphere. Building parameters are given in **Table 3**.

Table 3 Printing parameters

Power (W)	Scanning Speed (mm/s)	Layer thickness (µm)	Hatch Spacing (µm)	Laser Diameter (µm)	Volumetric energy density (J/mm^3)
220	300	30	60	60	407

The samples were printed directly onto the H13 base plate. Due to the nature of the machine, the preheated samples were left to air cool within the printing chamber. They were removed from the base plate via electro-discharge machining. Afterward, they have machined into 10 mm x 10 mm x 55 mm Charpy specimens (kv_2). The samples were tempered at 4 temperatures:

- As build state.
- Tempered at 450 °C for 2 hours.
- Tempered at 500 °C for 2 hours.
- Tempered at 550 °C for 2 hours.
- Tempered at 650 °C for 2 hours.

Impact toughness (SIST EN ISO 148 – 1: 2017) was measured on a MLF system, PSW 300 at room temperature. Lastly, Rockwell hardness was measured on an Instron B2000 (Illinois Tool Works, Norwood, Massachusetts, USA).

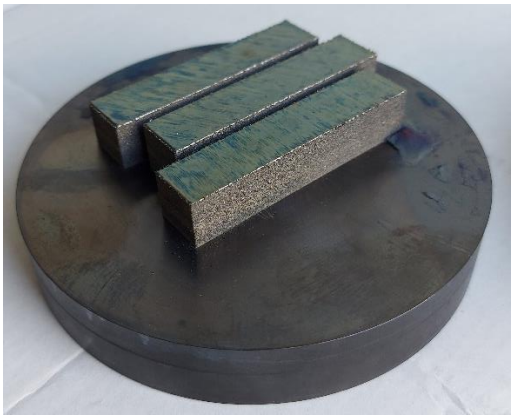

Figure 1 LPBF-produced H13 samples still attached to the baseplate.

All of the samples were cut along the build direction, mounted in Bakelite resin then ground, polished, and etched using Villela's reagent (1 gram of picric acid and 5 ml hydrochloric acid to 100 ml of ethanol) to reveal the microstructure. The samples were observed under a light microscope (Nikon Microphot-FXA, Nikon, Tokyo, Japan) equipped with an Olympus DP73 digital camera (Olympus, Tokyo, Japan) and a ZEISS CrossBeam 550 FIBSEM (ZEISS, Oberkochen, Germany) scanning electron microscope to determine the porosity and microstructure of the samples.

2.2. Conventionally produced samples

The conventionally produced samples were cut into 10x10x55 mm Charpy specimens (kv_2). They were austinized in a vacuum furnace at 1050 °C where they were held at the temperature for 20 minutes. Afterward, the samples underwent four different tempering treatments:

- tempered at 450 °C for 2 hours.
- tempered at 500 °C for 2 hours.
- tempered at 550 °C for 2 hours.
- tempered at 600 °C for 2 hours.

Impact toughness and Rockwell hardness were measured on the same devices as the printed samples. Their microstructure was also investigated using the aforementioned SEM.

3. RESULTS

When observed under a light microscope, remnants of the melt pools are visible (**Figure 2**). This is typical for LPBF-produced parts, as the laser melts and re-melts certain parts of the material, leaving behind these tracks. This is in line with our prior research [10]. The material also looks mostly dense, however, the optical method for determining part density is not the most accurate for accessing porosity, as it only observes a single layer of material, potentially not detecting porosities residing in other parts of the sample. When observed under SEM, a columnar grain structure is evident (**Figure 3 b)** and **c)**). This is also typical for AM-manufactured parts, as the grains tend to grow along the direction of heat flow, which is the build direction [11]. It is also important to mention, that the sample in the as-built stage has few to no visible carbides. This is due to the high cooling speed, associated with LPBF, which does not allow for carbides to precipitate during the printing process. However, in the tempered sample, small carbides are visible, as the thempering process allowed for enough

diffusion to occour, for them to precipitate. This is in comparison to the classically produced sample (**Figure 3 a)**), which has more noticeable, courser carbides.

Figure 2 melt pools observed with light microscopy

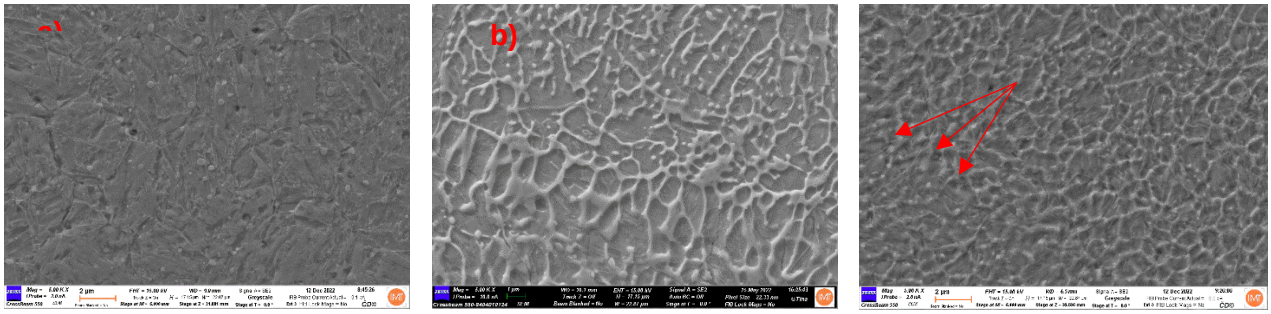

Figure 3 SEM images of the H13 samples: a) reference material in the quenched and tempered state; b) Sample manufactured with LPBF at 350 °C of preheating in the as-built state; c) Sample manufactured with LPBF at 350 °C tempered at 500 °C for 2 hours

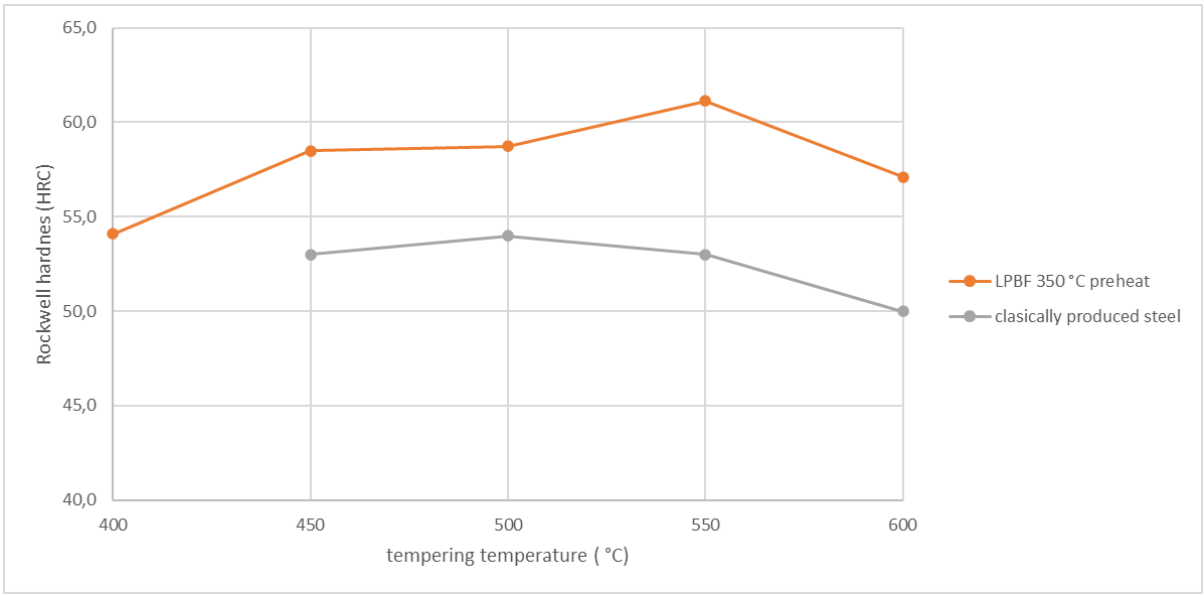

Figure 4 Rockwell hardness of the LPBF samples compared to classically produced samples at various tempering temperatures

The Rockwell hardness test determined, that the samples made with LPBF had higher hardness at all tempering temperatures **Figure 4**. This can be attributed to the smaller grain size obtained by the fast cooling rate of the LPBF process and the precipitation of finer carbides, than those in the classically produced sample. Furthermore, the LPBF samples exhibit a secondary hardness peak at a higher temperature than that of the classically produced samples. The reason behind this effect is unclear and needs further research, however, one explanation may be that the greater amount of fine carbides offers higher heat resistance [12].

Figure 5 Displays the impact toughness of the LPBF samples. The as-build samples have the lowest toughness because some retained stresses remain in the material. While the toughness increases with tempering temperature, the highest toughness (8 Jouls) is still significantly lower than that achieved by the 550 °C tempered classically produced part. One explanation for the low toughness is residual porosity. The printed samples were made with parameters optimized for smaller samples. This can lead to under-melting porosity remaining in the samples, significantly reducing toughness.

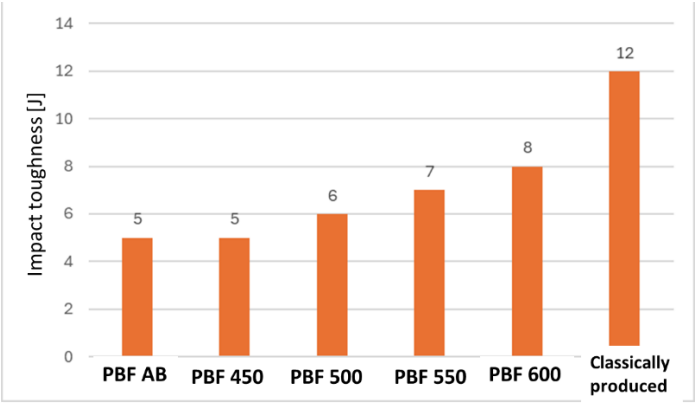

Figure 5 Impact toughness of LPBF samples compared to classically produced samples

4. CONCLUSIONS

Samples were produced via the LPBF method and tempered at different temperatures. The as-build samples contained very few carbides, as most of the carbide-forming elements are still in the super-saturated solid solution. The microstructure contains melt pools and a columnar grain structure, with small grains and and fine, dispersed carbides. The hardness of the printed parts can be higher than classically produced ones, with the secondary hardness peak occurring at higher temperatures. Toughness is lower in the printed samples, this is attributed to non-optimal parameters for the geometry and porosity.

Acknowledgments

This work was carried out within the framework of the Slovene research program P2-0132 and project L2-2613 funded by the Slovenian Research and Innovation Agency.

REFERENCES

[1] CHANTZIS, D., LIU, X., POLITIS, D.J., EL FAKIR, O., CHUA, T.Y., SHI, Z., WANG, L. Review on additive manufacturing of tooling for hot stamping. *Int. J. Adv. Manuf. Technol.* 2020, vol. *109*, pp. 87–107, doi:10.1007/s00170-020-05622-1.

[2] NARVAN, M., AL-RUBAIE, K.S., ELBESTAWI, M. Process-structure-property relationships of AISI H13 tool steel processed with selective laser melting. *Materials (Basel).* 2019, vol. *12*, pp. 1–20, doi:10.3390/ma12142284.

[3] ACKERMANN, M., ŠAFKA, J., VOLESKÝ, L., BOBEK, J., KONDAPALLY, J.R. Impact testing of H13 tool steel processed with use of selective laser melting technology. *Mater. Sci. Forum* 2018, vol. *919*, pp. 43–51, doi:10.4028/www.scientific.net/MSF.919.43.

[4] MINGUELLA-CANELA, J., MORALES PLANAS, S., DE MEDINA IGLESIAS, V.C., DE LOS SANTOS LÓPEZ, M.A. Quantitative analysis of the effects of incorporating laser powder bed fusion manufactured conformal cooling inserts in steel moulds over four types of defects of a commercially produced injected part. *J. Mater. Res. Technol.* 2023, vol. *23*, pp. 5423–5439, doi:10.1016/J.JMRT.2023.02.164.

[5] KAHLERT, M., VOLLMER, M., WEGENER, T., NIENDORF, T. On the fatigue behavior of a tool steel manufactured by powder bed based additive manufacturing—a comparison between electron- and laserbeam processed AISI H13. *Prog. Addit. Manuf.* 2024, pp. 1–14, doi:10.1007/S40964-024-00581-5/FIGURES/8.

[6] SUN, Y., WANG, J., LI, M., WANG, Y., LI, C., DAI, T., HAO, M., DING, H. Thermal and mechanical properties of selective laser melted and heat treated H13 hot work tool steel. *Mater. Des.* 2022, vol. *224*, 111295, doi:10.1016/J.MATDES.2022.111295.

[7] VILARDELL, A.M., HOSSEINI, S.B., ÅSBERG, M., DAHL-JENDELIN, A., KRAKHMALEV, P., OIKONOMOU, C., HATAMI, S. Evaluation of post-treatments of novel hot-work tool steel manufactured by laser powder bed fusion for aluminum die casting applications. *Mater. Sci. Eng. A* 2021,vol. *800*, pp. 132-137, doi:10.1016/j.msea.2020.140305.

[8] HE, Y., ZHONG, M., BEUTH, J., WEBLER, B. A study of microstructure and cracking behavior of H13 tool steel produced by laser powder bed fusion using single-tracks, multi-track pads, and 3D cubes. *J. Mater. Process. Technol.* 2020, vol. *286*, doi:10.1016/j.jmatprotec.2020.116802.

[9] ZHANG, J., SCHUMACHER, J., CLAUSEN, B. A comprehensive study on the influence of the scan pattern in two porosity levels and surface roughness on the fatigue behavior of laser powder bed fusion manufactured specimens made of steel H13. *J. Mater. Sci.* 2023, vol. *58*, pp. 10457–10483, doi:10.1007/S10853-023-08541-0/FIGURES/10.

[10] TOME, S.; KARPE, B.; PAULIN, I.; GODEC, M. *Effect of heat treatment on thermal conductivity of additively manufactured aisi H13 tool steel*. In: Proceeding of the 32th Int. Conf. METAL2023, Brno: Tanger, 2023 doi:10.37904/metal.2023.4677.

[11] DU, X., LIU, X., SHEN, Y., LIU, R., WEI, Y. H13 tool steel fabricated by wire arc additive manufacturing: Solidification mode, microstructure evolution mechanism and mechanical properties. *Mater. Sci. Eng. A* 2023, vol. *883*, 145536, doi:10.1016/J.MSEA.2023.145536.

[12] MOVCHAN, O. V; CHORNOIVANENKO, K.O. Secondary hardness and heat resistance of high-speed steels. *Prog. Phys. Met* 2020, vol. 21, doi:10.15407/ufm.21.01.072.